The correspondence between morphometric MRI and metabolic profile in Rasmussen's encephalitis

Chongyang Tang [a,1], Peng Ren [b,c,1], Kaiqiang Ma [a], Siyang Li [b,c], Xiongfei Wang [a], Yuguang Guan [a], Jian Zhou [a], Tianfu Li [d,e,f], Xia Liang [b,*], Guoming Luan [a,e,f,*]

[a] Department of Neurosurgery, SanBo Brain Hospital, Capital Medical University, Beijing 100093, China
[b] Laboratory for Space Environment and Physical Science, Harbin Institute of Technology, Harbin 150001, China
[c] School of Life Science and Technology, Harbin Institute of Technology, Harbin, 150001, China
[d] Department of Neurology, SanBo Brain Hospital, Capital Medical University, Beijing 100093, China
[e] Key Laboratory of Epilepsy, Beijing 100093, China
[f] Center of Epilepsy, Beijing Institute for Brain Disorders, Beijing 100093, China

ARTICLE INFO

ABSTRACT

Volumetric magnetic resonance imaging (MRI) atrophy is a hallmark of Rasmussen's encephalitis (RE). Here, we aim to investigate voxel-wise gray matter (GM) atrophy in RE, and its associations with glucose hypometabolism and neurotransmitter distribution utilizing MRI and PET data. In this study, fifteen RE patients and fourteen MRI normal subjects were included in this study. Voxel-wise GM volume and glucose metabolic uptake were evaluated using structural MRI and FDG-PET images, respectively. Spatial Spearman's correlation was performed between GM atrophy of RE with FDG uptake alterations, and neurotransmitter distributions provided in the JuSpace toolbox. Compared with the control group, RE patients displayed extensive GM volume loss not only in the ipsilateral hemisphere, but also in the frontal lobe, basal ganglia, and cerebellum in the contralateral hemisphere. Within the RE group, the insular and temporal cortices exhibited significantly more GM atrophy on the ipsilesional than the contralesional side. FDG-PET data revealed significant hypometabolism in areas surrounding the insular cortices in the ipsilesional hemisphere. RE-related GM volumetric atrophy was spatially correlated with hypomebolism in FDG uptake, and with spatial distribution of the dopaminergic and serotonergic neurotransmitter systems. The spatial concordance of morphological changes with metabolic abnormalities suggest FDG-PET offers potential value for RE diagnosis. The GM alterations associated with neurotransmitter distribution map could provide novel insight in understanding the neuropathological mechanisms and clinical feature of RE.

1. Introduction

Rasmussen's encephalitis (RE) is a rare progressive disease that typically starts in childhood. Its clinical characteristic representations include refractory epilepsy, and progressive neurological and cognitive impairments, with progressive atrophy of the unilateral hemisphere (Varadkar et al., 2014). In most cases, epileptic seizures that mark the onset of RE in most cases gradually develop into refractory seizures in response to anti-seizure drugs (ASDs), and can eventually progress into epilepsia partialis continua (EPC) in a portion of patients(Tang et al., 2020). Hemispherectomy is currently a satisfactory therapeutic strategy that can effectively inhibit seizures. In particular, disconnecting the hemispheres via surgery renders 70%–80% of patient seizure-free, yet it can result in hemiparesis and hemianopia(Guan et al., 2017). Although neuropathological and immunological studies in RE demonstrated severely disabling inflammation in the ipsilesional hemispheric cortex,

including T cell infiltration and microglial nodules associated with neuronal loss and astrogliosis, the pathogenesis and factors responsible for lateralization are not yet completely clear(He et al., 2020).

Currently, the diagnostic criteria for RE mainly depend on the European consensus statement proposed in 2005 by Bien et al(Bien et al., 2005), in which magnetic resonance imaging (MRI) appearances represent a vital condition for diagnosing RE. The characteristic MRI features include cortical swelling in the early phase of RE along with hyperintensity on T2-weighted and fluid-attenuated inversion recovery (FLAIR) images. Previous studies found preferential cerebral atrophy in the frontal lobe and the insula, followed by volume loss of the caudate nucleus as the disease progresses; eventually, the atrophy spreads to the entire ipsilesional cerebral hemisphere(Bien et al., 2002; Yamazaki et al., 2011). Volumetric MRI studies also revealed regional atrophy of the contralesional hemisphere in addition to the affected side using voxel-based morphometry (VBM) analysis, and the degree of hemispheric atrophy was found to be closely related with clinical and cognitive assessments(Rudebeck et al., 2018).

Fluorodeoxyglucose-positron emission tomography (FDG-PET) has been extensively applied in the preoperative evaluation of intractable epilepsy, with irregular metabolism suggesting neural network dysfunction. The relevance of FDG-PET to the localization value of ictal epileptic foci has been established(Strohm et al., 2019). Widespread hypometabolism on FDG-PET images corresponds with cerebral atrophy on MR images in the affected hemisphere in RE patients, suggesting that FDG-PET data may provide valuable information regarding increasing diagnostic confidence of RE(Fiorella et al., 2001). Therefore, establishing the link between FDG-PET hypometabolism and MRI volume atrophy may provide unique insights into understanding the clinical and neuropathological significance of these two neuroimaging characteristics in RE. However, to date, there have been very few cross-modal studies to explore whether and how hypometabolism would be associated with gray matter (GM) atrophy in RE.

Recent progress in the development of novel tracers for PET or single photon computed emission tomography (SPECT) has allowed for the quantification of specific neurotransmitter availability(Beliveau et al., 2017; Lehto et al., 2015). Based on these advances in molecular imaging, molecular atlases that map the anatomical distribution of a series of neurotransmitters, such as noradrenergic and serotonergic neurotransmitter systems, have been constructed using PET or SPECT, providing the possibility for investigating the neurotransmitter basis for neuroimaging abnormalities associated with neurological diseases(Dukart et al., 2018).

In the present study, we investigated GM atrophy and metabolic dysregulation in a cohort of patients with RE, and taking advantage of a publicly available resource characterizing the spatial distribution of multiple neurotransmitter systems, we aim to study whether and how the GM alterations in RE would be related to hypometablism and normal neurotransmitter distribution. We hypothesized that there would be a close relationship between GM atrophy and hypometabolism in RE patients, and the GM loss in RE patients would be associated with spatial distribution of specific neurotransmitter systems.

2. Materials and methods

2.1. Subjects

A total of 15 RE patients (10 females; mean age ± standard deviation [SD]: 90.80 ± 39.82 months) evaluated at the epilepsy center of the Sanbo Brain Hospital were included in the present study. The inclusion criteria were as follows: (1) RE patients diagnosed according to the diagnostic criteria of Bien et al. (Bien et al., 2005); and (2) childhood-onset RE patients. For the control group, we chose 14 controls with non-RE epilepsy from epilepsy center of the Sanbo Brain Hospital, with matching age (mean age ± SD: 108.07 ± 46.36 months) and gender (8 females) with the RE patients. All the controls with non-RE epilepsy had

negative (nonlesional) findings on MR scans and had clearly lateralizing epilepsy as documented by their video-electroencephalography monitoring. This retrospective study was approved by the Ethics Committee of the Sanbo Brain Hospital at Capital Medical University. All participants or their guardians signed the informed consent form.

2.2. Image acquisition

MRIs were acquired at two different imaging sites at our epilepsy center. Overall, 23 scans (14 RE scans, 9 control scans) were performed with a 1.5 T Philips Achieva scanner. The other 6 scans (1 RE scan, 5 control scans) were performed with a 3.0 T GE DISCOVERY MR750W scanner. The 3D volume T1-weighted Magnetization Prepared Rapid Acquisition with Gradient Echo (MPRAGE) sequence was used to obtain high-resolution anatomical images. The 1.5 T scanner sequence parameters were as follows: echo time (TE) = 9.2 ms (ms), repetition time (TR) = 25 ms, flip angle (FA) = 30 degrees, matrix = 256 × 256, field of view (FOV) = 100, slice thickness = 0.94 mm, slices = 213. The 3.0 T scanner sequence parameters were as follows: TE = 3.2 ms, TR = 8.7 ms, and FA = 12 degrees, matrix = 256 × 256, FOV = 100, slice thickness = 1 mm, slices = 176. The scanner effect is included as a covariate throughout the analysis.

The RE patients also underwent FDG-PET. All patients fasted for at least 6 h and had normal blood glucose levels before undergoing the procedure. The participants underwent brain PET and CT scans (GE Medical Systems) in 8 min, 1 h after receiving an intravenous injection of [18F] FDG (dose: 0.15 mCi/kg).

2.3. MRI and PET image processing

All images were checked and flipped as needed to ensure that the ipsilesional hemisphere was located on the same side. MRI images were preprocessed and whole-brain VBM analysis was conducted using the Computational Anatomy Toolbox (CAT12; http://dbm.neuro.uni-jena.de/cat.html) for Statistic Parametric Mapping (SPM) version 12 (http://www.fil.ion.ucl.ac.uk/spm) on MATLAB R2016a (MathWorks, Natick, MA). Following the customized pipeline for pediatric data outlined in the CAT12 manual, a customized tissue probability map (TPM) and diffeomorphic anatomical registration through exponentiated Lie (DARTEL) algebra templates were created with the CerebroMatic toolbox for our age range first, then the images were segmented into GM, white matter (WM), and cerebrospinal fluid (CSF) by a unified tissue segmentation procedure(Wilke et al., 2017). The segmented GM images were spatially normalized to the DARTEL space and modulated by the Jacobian determinant derived from the spatial normalization by DARTEL. Finally, the processed GM data were smoothed using Gaussian kernel-processed GM data with an 8 mm full width half maximum (Ashburner, 2007). The total intracranial volume (TIV) was also estimated for each participant and was later used as a covariate.

FDG-PET images were co-registered to the original MRI T1 image and were then spatially normalized to the International Consortium for Brain Mapping (ICBM) standard space using a transformation matrix from the MRI normalization procedure achieved via SPM12. A reference region comprised of the cerebellar vermis and pons was identified for each subject using the automated anatomical labeling (AAL) atlas and manual editing(Tzourio-Mazoyer et al., 2002). PET images were intensity normalized to the median uptake and smoothed with an 8 mm full width at half maximum Gaussian kernel.

2.4. Volumetric MRI comparison analysis

To assess the volumetric group differences, we first performed a t-test between the RE and control groups using Statistical nonParametric Mapping 13 (SnPM13, http://warwick.ac.uk/snpm) toolbox from SPM12 with 5,000 permutations(Nichols and Holmes, 2002). Age, gender, and TIV were taken as covariates. A two-tailed test with voxel-

level $P < 0.01$ and cluster-level $P < 0.05$ thresholds at each side were used.

To assess the GM volumetric alterations of RE patients between the ipsilesional and contralesional hemispheres, we also conducted a paired *t*-test of GM volume using SnPM using the same two-level threshold.

2.5. Metabolic FDG-PET comparison analysis

Since FDG-PET data were only acquired in the RE patients, we evaluated metabolic alterations by comparing FDG-PET uptake values between the ipsilesional and contralesional hemispheres in RE patients under voxel-wise FWE corrected $P < 0.05$ threshold.

2.6. Spatial correlation analysis between volumetric MRI and metabolic FDG-PET changes

To explore cross-modal spatial correspondence between volumetric alterations of GM and glucose hypometabolism in RE patients, spearman's correlation analysis was performed at two levels: (1) voxel-wise correlation between GM volume and FDG-PET uptake in RE group; (2) region-wise correlation of ipsilesion versus contralesion alternations between GM volume and FDG-PET uptake in RE group across 123 brain regions from the Brainnetome Atlas (http://atlas.brainnetome.org) (Fan et al., 2016). The region-wise analysis was also validated using only GM areas showing significant volume change in RE versus control contrast.

2.7. Neurotransmitter correlates of volumetric and metabolic changes in RE patients

To evaluate the neurotransmitter basis underlying regional vulnerability of GM atrophy in RE patients, we extracted region-wise neurotransmitter distribution from the JuSpace toolbox (https://github.com/juryxy/JuSpace), which included dopaminergic, serotonergic, noradrenergic, and GABAergic neurotransmission (Dukart et al., 2021). For each extracted neurotransmitter distribution map, we computed its Spearman's rank correlations with between-group GM atrophy or ipsilesional versus contralesional GM alteration map in RE patients, respectively. A threshold with FDR corrected $P < 0.05$ was considered significant.

2.8. Associations between volumetric and metabolic changes with clinical assessments in RE patients

To explore the relationship between clinical characteristics and GM volume or glucose metabolic alternation, we performed voxel-wise correlations between GM volume or FDG-PET uptake value with clinical indices, including EPC and duration of neurological deficits. Age, gender and TIV were also regressed and significant threshold was set at $P < 0.05$ with FWE correction.

3. Results

3.1. Patients demographics

Tables 1 and S1 summarized the clinical features of all RE participates and MRI-normal controls in this study. All of the patients underwent preoperative evaluation and surgical management for their identified neuropathology of RE. An example of the preoperative MRI images and postoperative pathological features of one patient are shown in Supplementary Fig. 1. No significant group differences were found in age or gender.

3.2. Volumetric MRI changes in RE patients

Fig. 1A shows the extensive atrophic GM distributed in the cortical and subcortical areas as compared to controls. Regions of extensive and

Table 1
Demographics and clinical details of RE patients

	RE group	Control group	P-value
n	15	14	–
Gender (M/F)	5/10	6/8	P=0.597[a]
AS (m, mean±SD)	90.80±39.82	-	–
IH (L/R)	9/6	-	–
AFS (m, mean±SD)	64.67±21.98	-	–
I1 (m, mean±SD)	10.30±11.39	-	–
I2 (m, mean±SD)	15.13±16.43	-	–
I3 (m, mean±SD)	26.13±30.66	-	–

IH = Ipsilateral hemisphere; AS = Age at surgery; AFS = Age at first seizure; I1 = Interval between seizure onset and EPC onset; I2 = Interval between seizure onset and neurological deficit; I3= Interval between seizure onset and MRI scan; SD = standard deviation; L = Left; R = Right; M = Male; F = Female; m = month.
[a] No significant group difference using chi-square test.

significant volumetric loss occurred in each lobe of the ipsilesional hemisphere, most obviously in the frontal lobe, temporal lobe, parietal lobe, and insula. In the contralateral hemisphere, areas in the basal and medial frontal cortex also displayed lower GM volumes. The subcortical basal ganglia and cerebellar regions exhibited bilateral GM volume loss.

Further, since RE is clinically characterized by unilateral lesions in the cerebral cortex and other structures, we compared the GM volume between the affected and the unaffected hemispheres to evaluate within-group ipsilesional atrophy. Our results identified that the ipsilesional–contralesional GM alterations were limited to the ipsilesional hemisphere of RE (Fig. 1B). Specifically, the ipsilesional hemisphere of RE patients exhibited significantly lower GM volume in regions of the insular cortex, and temporal, parietal, and occipital cortices. Moreover, higher GM volumes were evident in the cerebellar cortex of the ipsilesional hemisphere in contrast to the contralesional hemisphere.

3.3. Correlation between volumetric MRI and metabolic FDG-PET changes

The FDG-PET images of RE patients were voxel-wise analyzed to evaluate glucose metabolism alterations. Compared with the contralateral hemisphere, the ipsilesional hemisphere showed extensive areas of reduced uptake, except for a cluster in the cerebellum, which exhibited hypermetabolism (uncorrected voxel-wise $P < 0.05$; Supplementary Fig. 2). With a relatively stringent significance threshold (uncorrected voxel-wise $P < 0.01$), Fig. 2A illustrates the hypometabolic clusters of the ipsilesional hemisphere distributed in the insular cortex and its surrounding cortices in RE.

We next inquired into whether the structural images of RE were related to glucose metabolic images of the cortical and subcortical structures based on a region-wise parcellation atlas (BNA atlas; 246 regions). Fig. 2B demonstrates that there were significant positive correlations between volumetric MRI and metabolic FDG-PET ($R = 0.31$, $P = 0.0005$) across the entire ipsilesional hemisphere during ipsilesion versus contralesion comparisons. Moreover, the clear MRI–PET correlations were repeated across brain areas with significant volumetric MRI atrophy ($R = 0.63$, $P = 1.3e-09$; Fig. 2C). The statistical map of the whole GM voxel-wise analysis showed similar positive spatial correspondence between GM volume and FDG-PET uptake in the ipsilesional hemisphere across RE subjects (Supplementary Fig. 3).

3.4. Spatial correlation of GM atrophy with neurotransmitter distribution

We computed the spatial correspondence between GM volumetric loss in RE and 12 different PET- or SPECT-derived normal neurotransmitter distribution maps using the JuSpace toolbox. The GM atrophy in RE patients was significantly associated with the spatial distribution of the 5HT1a ($\rho = -0.23$, $P = 0.036$), D1 ($\rho = -0.32$, $P = 0.003$), DAT ($\rho =$
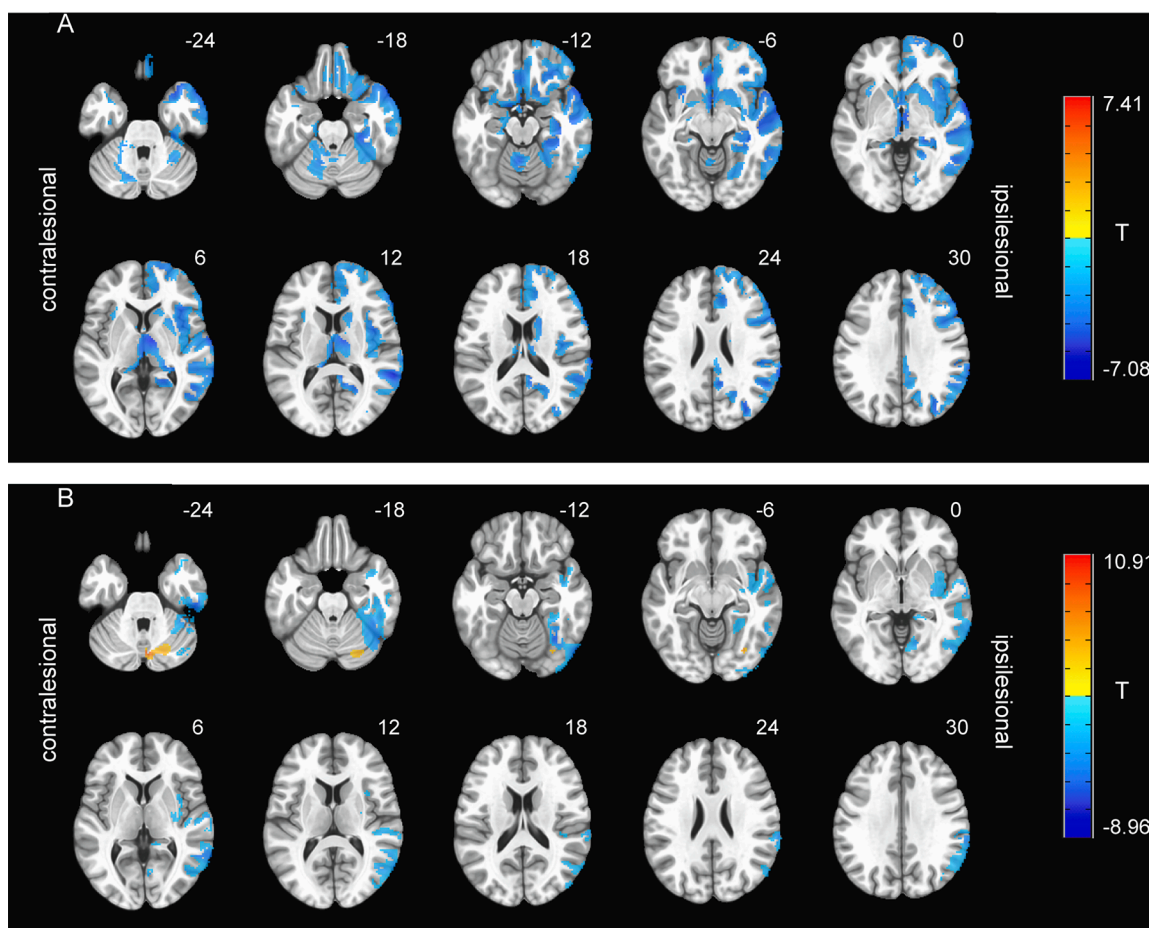
Fig. 1. Volumetric MRI changes of RE patients. (A) A comparison of the MRI scans of 15 RE patients and 14 controls indicated extensive gray matter (GM) atrophy distributed in cortical and subcortical areas (blue). (B) The comparison between the ipsilesional and contralesional hemispheres indicated lower cortical GM volume in the temporal lobe, insula, parietal lobe, and occipital lobe (blue). The cerebellar cortex showed the greater cortical volume (red–yellow). Two-tailed tests with voxel-level $P < 0.01$ and cluster-level $P < 0.025$ at each side thresholds were applied for visualization.
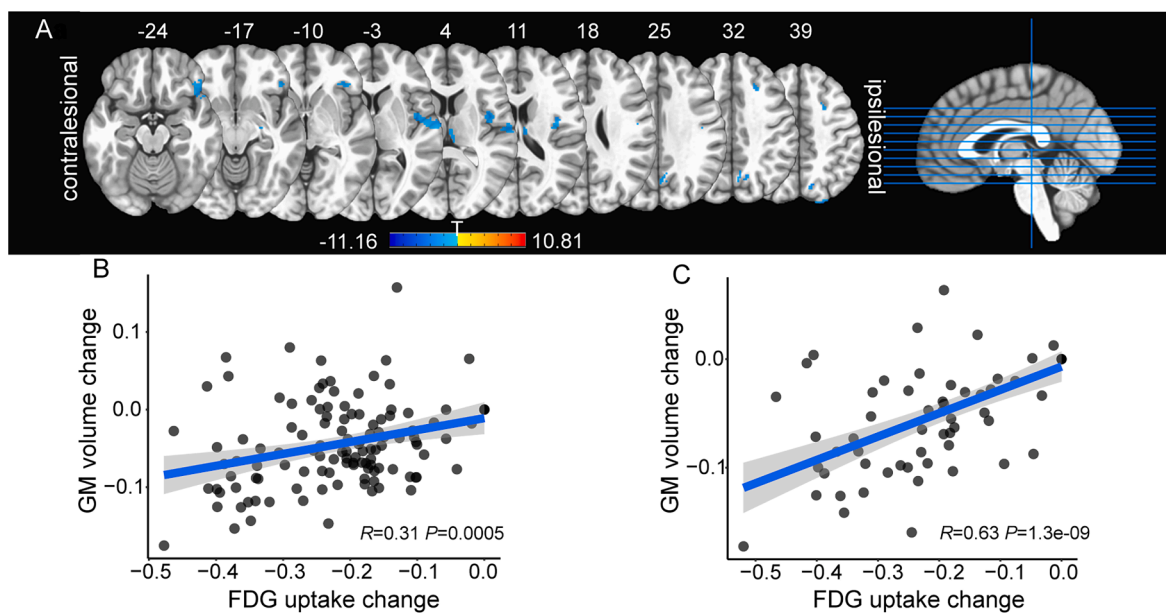

Fig. 2. Abnormal uptake of FDG-PET in RE, and the association between volumetric MRI and metabolic FDG-PET. (A) The ipsilesional hemisphere demonstrated significant hypometabolic clusters mainly in the insula and surrounding areas compared with the contralesional hemisphere (blue). (B–C) Voxel-wise FWE corrected $P < 0.05$ threshold was taken hemispherical volumetric MRI and metabolic FDG-PET alternation showed positive correlations (B) across the entire ipsilesional hemisphere GM, and (C) across the brain areas with significant volumetric MRI alternation.

-0.23, $P = 0.036$), MU ($\rho = -0.31$, $P = 0.003$), and SERT-DASB ($\rho = -0.22$, $P = 0.043$) maps (Fig. 3A). Moreover, the ipsilesional–contralesional GM alterations in RE patients were correlated significantly with the spatial distribution of 7 different neurotransmitter maps (Fig. 3B), including 5HT1a ($\rho = -0.43$, $P = 0.003$), 5HT2a ($\rho = -0.31$, $P = 0.027$), D1 ($\rho = -0.52$, $P = 0.0003$), D2 ($\rho = -0.38$, $P = 0.005$), DAT ($\rho = -0.4$, $P = 0.005$), SERT-DASB ($\rho = -0.4$, $P = 0.005$), and SERT-MADAM ($\rho = -0.39$, $P = 0.005$). In sum, the dopaminergic (D1, DAT, SERT-DASB) and serotonergic (5HT1a) neurotransmitters exhibited significant relevance for GM volumetric alterations in RE (Supplementary Fig. 4–5).

3.5. Relationship with clinical characteristics

We explored the relationship between clinical variables and the hemispheric GM volume or FDG uptake in RE patients. No statistically significant correlation between GM volume or FDG uptake with disease duration were found. Likewise, no significant correlations were found for the duration of EPC and duration of neurological deficits.

4. Discussion

In this study, we investigated the relationship between morphometric MRI brain regions and cerebral metabolic degeneration in a group of 15 RE patients. We described the distribution of volumetric alterations in a cohort of RE, which included atrophic clusters located in the insular cortex, temporal lobe, and parietal lobe of the ipsilateral hemisphere. Significant positive correlations were found in the brain region featuring volumetric MRI atrophy and hypometabolic FDG-PET. We also found a significant spatial, region-wise correlation between MRI alterations and neurotransmitter mapping in the dopaminergic and serotonergic systems. These results provide evidence linking GM atrophy with hypometabolism in RE, and its potential neurotransmitter substrate.

MRI studies of RE, as characterized by progressive atrophy, have progressed from using descriptive pattern recognition to automatic voxel-based volumetric measurement on MRI images(Chiapparini et al., 2003; David et al., 2019; Pradeep et al., 2014; Takeoka et al., 2003; Wang et al., 2016). The present study found voxel-based volumetric alterations using two analytic strategies: one that compared the GM volume between RE patients and control patients, and the other that contrasted ipsilesional and contralesional hemispheres in RE patients. Both strategies revealed consistent GM atrophy across extensive cortical structures in the ipsilesional hemisphere, especially the insular and its extended temporal cortices. Automated MRI volumetric method has already been used to determine the brain volume loss of RE in several previous studies. In a previous study, the insula was found to show significantly more atrophy compared with all the other cortical regions in the affected hemisphere of RE patients compared to healthy controls and non-RE epilepsy patients(Wang et al., 2016). In another study by Wagner et al., 12 RE patients were retrospectively analyzed and the findings indicated that the atrophy was preferentially pronounced in the frontal lobe and insula of the ipsilateral hemisphere(Wagner et al., 2012). All of the above findings demonstrated that although the automated MRI volumetric method partly varied from our approach given the different template and calculated algorithm used, the ipsilateral area of the insula appeared to show the most significant GM volume loss in RE patients, which is consistent with our present findings. It is worth to explore the diagnostic value of GM atrophy in insula in RE patients in future studies.

Comparing with the control patients, we also found significant GM volume loss in the frontal lobe and subcortical caudate nucleus in the contralesional hemisphere in RE patients. Recent studies have revealed that the cortical and subcortical GM structures of both the affected and unaffected hemispheres demonstrated progressive volume reduction compared with healthy controls, which is generally concordant with our results(David et al., 2019; Rudebeck et al., 2018). We note that the volumetric atrophy in the contralesional hemisphere may likely due to a secondary neurodegeneration of the ipsilesional GM loss rather than bihemispheric pathology, which warrants future investigations. Other studies also found GM atrophy in the brainstem, thalamus and perisylvian regions in the unaffected hemisphere(David et al., 2019; Rudebeck et al., 2018), which were found to appear intact in our present results. The inconsistencies in the GM atrophy of RE may be due to the selection of RE patients and control subjects. Another factor that may underly the discrepancy among studies is the difference in disease progression. Previous studies have focused on different periods of RE duration which ranged from 3.8 to 10.19 years from seizure onset to MRI scan(David et al., 2019; Rudebeck et al., 2018). In contrast, to provide a
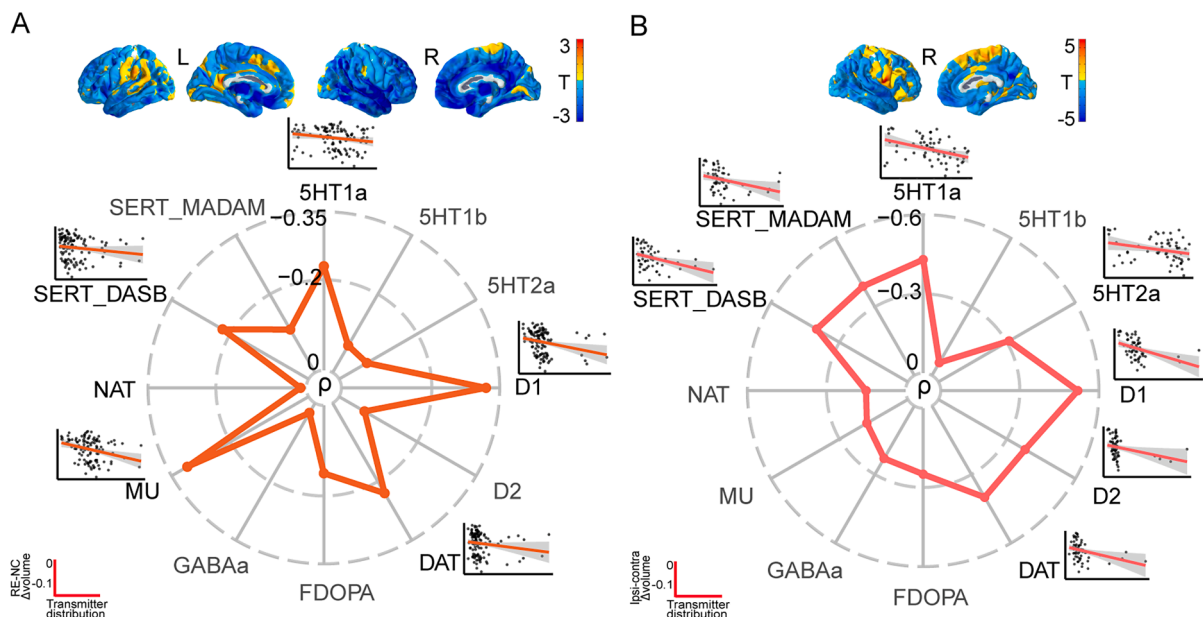

Fig. 3. Spatial correlation between MRI alternation and nuclear imaging-derived neurotransmitter distribution. The GM alterations (surface demonstration at the top) induced by (A) RE–control or (B) ipsilesional–contralesional comparisons were significantly associated with the spatial distribution of dopaminergic and serotonergic neurotransmitter maps, respectively. Scatter plot were showed only for significant correlations under FDR corrected $P < 0.05$ threshold.

relatively more homogeneous characterization of RE patients, the present study chose to examine RE subjects with a mean duration of 2.18 years. It is vital to note that atrophic changes were connected with disease progress.

In an earlier study, researchers observed extensive unilateral cerebral hypometabolism in FDG-PET, but only via specialist observations, which coincided with cerebral MRI atrophy in RE(Fiorella et al., 2001). Although metabolic imaging is not part of any condition in Bien's (2005) diagnostic criteria, the abnormal uptake of cerebral blood flow (CBF)-SPECT, central benzodiazepine receptor (BZR)-SPECT, and FDG-PET occurred during a regular stage of RE(Banati et al., 1999; Tessonnier et al., 2009; Wang et al., 2013). Previous research has indicated that the abnormality identified by BZR-SPECT and FDG-PET through the visual assessment appeared before the MRI volume changes occurred, and might show an even stronger relationship to the ictal onset area identified by ictal EEG(Kuki et al., 2018). Brain FDG-PET has highlighted the significant value of central nervous system diseases, particularly epilepsy related to limbic encephalitis epilepsy or new-onset refractory status epilepticus, whereas descriptive pattern observations or voxel-based analysis approach were used(Dodich et al., 2016; Strohm et al., 2019). To our knowledge, this is the first study to quantitatively determine the relationship between structural and metabolic abnormalities in RE patients. The definite correspondence between MRI and PET might provide potential value for RE diagnosis.

The JuSpace toolbox provides an effective means through which to connect neuroimaging and neurotransmitter information, and its reliability has been recently verified(Dukart et al., 2021). Our results suggest that in RE patients, GM alternations across either RE–control whole-brain comparisons or ipsilateral–contralateral comparisons were significantly correlated with the intrinsic distribution of multiple neurotransmitters, which revealed potential neurotransmitter basis of regional vulnerability. These significant correlations indicate that atrophic changes may occur preferentially in brain regions that are rich in dopaminergic (D1, DAT, SERT-DASB) and serotonergic (5HT1a) neurotransmitters. Although JuSpace is used to detect the correlation between the spatial structure of imaging alterations and the availability of a specific receptor across the brain, the templates of PET/SPECT-derived neurotransmitters map for analysis come from healthy adult volunteers. Our results only indicated possible neurotransmitter risks related with regional atrophic vulnerability to RE and the answer to how the neurotransmitters are altered in RE needs future efforts.

Extensive researches have demonstrated the role of dopaminergic and serotonergic circuits in the epileptogenesis and control of seizure (Bozzi and Borrelli, 2013; Tripathi and Bozzi, 2015). Different types of dopaminergic and serotonergic receptors, localized on the neocortical and hippocampal nerve terminals, could prominently modulate the balance of excitatory neural network. Evidence showed that the expression of 5-HT1a receptor is associated with most of epileptogenic network and activation of 5-HT1a receptor through selective serotonin reuptake inhibitors had inhibitory effect on convulsive seizures(Arbabi Jahan et al., 2018). Studies on mice lacking specific D1 and D2 receptor subtypes showed that activation of D1 receptor promoted epileptogenic, whereas D2 receptor played the opposite role. The physiological balance of dopaminergic activity was essential to the complex neuromodulatory response to epileptogenesis(Bozzi and Borrelli, 2013; Bozzi et al., 2000; Gangarossa et al., 2014). Building on these prior studies, our results confirmed the critical role of dopaminergic and serotonergic activities in the pathogenesis of refractory epilepsy, and provided new insight suggesting that the normative spatial distribution of these neurotransmitters may contribute to the heterogenous regional vulnerability in brain atrophic changes in RE, and represent as potential risk factors promoting epileptogenesis. Future studies that explore how the distribution and activity of these neurotransmitters are altered in patients with RE may provide a more comprehensive understanding of their roles in epileptogenesis and potential direction for epilepsy treatment of RE.

Several limitations were summarized in this research. First, given that RE is a very rare disease, estimated as 2.4 cases/10^7 people $\leq$ age 18/year(Bien et al., 2013), the sample size used here is relatively small. Nevertheless, the study is sufficiently powered (83.974% with α level set at 0.01) as indicated by the statistical power calculation (PASS 15 software, https://www.ncss.com). Second, MRI images of the recruited participants were acquired on two different scanners, which might induce inevitable systematic bias. To mitigate this potential bias, we included the scanner effect as a covariate throughout the analysis. Future studies using single-scanner data with sufficient sample size could validate the current findings with greater study power. Third, the long-term trajectories of MRI atrophy development and metabolic alterations await further study, particularly when exploring longitudinal correlation analyses. Fourth, MRI-negative epilepsy patients were used as control subjects, while there might be slight volume changes compared with healthy subjects. Although ipsilesional versus contralesional comparisons were conducted in the present study to mitigate this possible impact on the overall results, future studies using age-matched healthy subjects as control subjects should be conducted.

In summary, we described the distribution of volumetric alterations in a cohort of RE by comparing differences with controls, which included atrophic voxel clusters located in the insular cortex, temporal lobe, and parietal lobe of the ipsilateral hemisphere. Moreover, volumetric GM loss was irrelevant in terms of clinical parameters. A trend towards a positive correlation was found in the brain region featuring volumetric MRI atrophy and hypometabolic FDG-PET. Although the MRI atrophy is one of the diagnostic standards in RE, our study about spatial concordance of MRI changes with glucose hypometabolism abnormalities suggest FDG-PET offers potential value for RE diagnosis. We also found a significant spatial, region-wise correlation between MRI alterations and neurotransmitter mapping in the dopaminergic and serotonergic systems. This information effectively links neuroimaging and underlying neurotransmitter patterns in RE. The study of these neurotransmitters in atrophic brain region are beneficial for understanding the pathological features and clinical treatment of RE.

CRediT authorship contribution statement

Chongyang Tang: Conceptualization, Methodology, Writing – original draft. **Peng Ren:** Conceptualization, Software, Formal analysis, Visualization, Writing – original draft. **Kaiqiang Ma:** Data curation, Formal analysis. **Siyang Li:** Software, Visualization. **Xiongfei Wang:** Data curation, Funding acquisition. **Yuguang Guan:** Data curation. **Jian Zhou:** Data curation. **Tianfu Li:** Data curation. **Xia Liang:** Conceptualization, Methodology, Funding acquisition, Writing – review & editing. **Guoming Luan:** Conceptualization, Funding acquisition, Supervision, Writing – review & editing.

Declaration of Competing Interest

The authors declare that they have no known competing financial interests or personal relationships that could have appeared to influence the work reported in this paper.

Appendix A. Supplementary data

Supplementary data to this article can be found online at https://doi.org/10.1016/j.nicl.2021.102918.

References

Arbabi Jahan, A., Rad, A., Ghanbarabadi, M., Amin, B., Mohammad-Zadeh, M., 2018. The role of serotonin and its receptors on the anticonvulsant effect of curcumin in pentylenetetrazol-induced seizures. Life Sci 211, 252–260.

Ashburner, J., 2007. A fast diffeomorphic image registration algorithm. NeuroImage 38, 95–113.

Banati, R.B., Goerres, G.W., Myers, R., Gunn, R.N., Turkheimer, F.E., Kreutzberg, G.W., Brooks, D.J., Jones, T., Duncan, J.S., 1999. [11C](R)-PK11195 positron emission tomography imaging of activated microglia in vivo in Rasmussen's encephalitis. Neurology 53, 2199–2203.

Beliveau, V., Ganz, M., Feng, L., Ozenne, B., Hojgaard, L., Fisher, P.M., Svarer, C., Greve, D.N., Knudsen, G.M., 2017. A High-Resolution In Vivo Atlas of the Human Brain's Serotonin System. J Neurosci 37, 120–128.

Bien, C.G., Granata, T., Antozzi, C., Cross, J.H., Dulac, O., Kurthen, M., Lassmann, H., Mantegazza, R., Villemure, J.G., Spreafico, R., Elger, C.E., 2005. Pathogenesis, diagnosis and treatment of Rasmussen encephalitis: a European consensus statement. Brain 128, 454–471.

Bien, C.G., Tiemeier, H., Sassen, R., Kuczaty, S., Urbach, H., von Lehe, M., Becker, A.J., Bast, T., Herkenrath, P., Karenfort, M., Kruse, B., Kurlemann, G., Rona, S., Schubert-Bast, S., Vieker, S., Vlaho, S., Wilken, B., Elger, C.E., 2013. Rasmussen encephalitis: incidence and course under randomized therapy with tacrolimus or intravenous immunoglobulins. Epilepsia 54, 543–550.

Bien, C.G., Urbach, H., Deckert, M., Schramm, J., Wiestler, O.D., Lassmann, H., Elger, C.E., 2002. Diagnosis and staging of Rasmussen's encephalitis by serial MRI and histopathology. Neurology 58, 250–257.

Bozzi, Y., Borrelli, E., 2013. The role of dopamine signaling in epileptogenesis. Front Cell Neurosci 7, 157.

Bozzi, Y., Vallone, D., Borrelli, E., 2000. Neuroprotective role of dopamine against hippocampal cell death. J Neurosci 20, 8643–8649.

Chiapparini, L., Granata, T., Farina, L., Ciceri, E., Erbetta, A., Ragona, F., Freri, E., Fusco, L., Gobbi, G., Capovilla, G., Tassi, L., Giordano, L., Viri, M., Dalla Bernardina, B., Spreafico, R., Savoiardo, M., 2003. Diagnostic imaging in 13 cases of Rasmussen's encephalitis: can early MRI suggest the diagnosis? Neuroradiology 45, 171–183.

David, B., Prillwitz, C.C., Hoppe, C., Sassen, R., Horsch, S., Weber, B., Hattingen, E., Elger, C.E., Ruber, T., 2019. Morphometric MRI findings challenge the concept of the "unaffected" hemisphere in Rasmussen encephalitis. Epilepsia 60, e40–e46.

Dodich, A., Cerami, C., Iannaccone, S., Marcone, A., Alongi, P., Crespi, C., Canessa, N., Andreetta, F., Falini, A., Cappa, S.F., Perani, D., 2016. Neuropsychological and FDG-PET profiles in VGKC autoimmune limbic encephalitis. Brain Cogn 108, 81–87.

Dukart, J., Holiga, S., Chatham, C., Hawkins, P., Forsyth, A., McMillan, R., Myers, J., Lingford-Hughes, A.R., Nutt, D.J., Merlo-Pich, E., Risterucci, C., Boak, L., Umbricht, D., Schobel, S., Liu, T., Mehta, M.A., Zelaya, F.O., Williams, S.C., Brown, G., Paulus, M., Honey, G.D., Muthukumaraswamy, S., Hipp, J., Bertolino, A., Sambataro, F., 2018. Cerebral blood flow predicts differential neurotransmitter activity. Sci Rep 8, 4074.

Dukart, J., Holiga, S., Rullmann, M., Lanzenberger, R., Hawkins, P.C.T., Mehta, M.A., Hesse, S., Barthel, H., Sabri, O., Jech, R., Eickhoff, S.B., 2021. JuSpace: A tool for spatial correlation analyses of magnetic resonance imaging data with nuclear imaging derived neurotransmitter maps. Hum Brain Mapp 42, 555–566.

Fan, L., Li, H., Zhuo, J., Zhang, Y., Wang, J., Chen, L., Yang, Z., Chu, C., Xie, S., Laird, A. R., Fox, P.T., Eickhoff, S.B., Yu, C., Jiang, T., 2016. The Human Brainnetome Atlas: A New Brain Atlas Based on Connectional Architecture. Cereb Cortex 26, 3508–3526.

Fiorella, D.J., Provenzale, J.M., Coleman, R.E., Crain, B.J., Al-Sugair, A.A., 2001. (18)F-fluorodeoxyglucose positron emission tomography and MR imaging findings in Rasmussen encephalitis. AJNR Am J Neuroradiol 22, 1291–1299.

Gangarossa, G., Ceolin, L., Paucard, A., Lerner-Natoli, M., Perroy, J., Fagni, L., Valjent, E., 2014. Repeated stimulation of dopamine D1-like receptor and hyperactivation of mTOR signaling lead to generalized seizures, altered dentate gyrus plasticity, and memory deficits. Hippocampus 24, 1466–1481.

Guan, Y., Chen, S., Liu, C., Du, X., Zhang, Y., Chen, S., Wang, J., Li, T., Luan, G., 2017. Timing and type of hemispherectomy for Rasmussen's encephalitis: Analysis of 45 patients. Epilepsy Res 132, 109–115.

He, X., Chen, F., Zhang, Y., Gao, Q., Guan, Y., Wang, J., Zhou, J., Zhai, F., Boison, D., Luan, G., Li, T., 2020. Upregulation of adenosine A2A receptor and downregulation of GLT1 is associated with neuronal cell death in Rasmussen's encephalitis. Brain Pathol 30, 246–260.

Kuki, I., Matsuda, K., Kubota, Y., Fukuyama, T., Takahashi, Y., Inoue, Y., Shintaku, H., 2018. Functional neuroimaging in Rasmussen syndrome. Epilepsy Res 140, 120–127.

Lehto, J., Johansson, J., Vuorilehto, L., Luoto, P., Arponen, E., Scheinin, H., Rouru, J., Scheinin, M., 2015. Sensitivity of [(11)C]ORM-13070 to increased extracellular noradrenaline in the CNS - a PET study in human subjects. Psychopharmacology (Berl) 232, 4169–4178.

Nichols, T.E., Holmes, A.P., 2002. Nonparametric permutation tests for functional neuroimaging: a primer with examples. Hum Brain Mapp 15, 1–25.

Pradeep, K., Sinha, S., Saini, J., Mahadevan, A., Arivazhagan, A., Bharath, R.D., Bindu, P. S., Jamuna, R., Rao, M.B., Chandramouli, B.A., Shankar, S.K., Satishchandra, P., 2014. Evolution of MRI changes in Rasmussen's encephalitis. Acta Neurol Scand 130, 253–259.

Rudebeck, S.R., Shavel-Jessop, S., Varadkar, S., Owen, T., Cross, J.H., Vargha-Khadem, F., Baldeweg, T., 2018. Pre- and postsurgical cognitive trajectories and quantitative MRI changes in Rasmussen syndrome. Epilepsia 59, 1210–1219.

Strohm, T., Steriade, C., Wu, G., Hantus, S., Rae-Grant, A., Larvie, M., 2019. FDG-PET and MRI in the Evolution of New-Onset Refractory Status Epilepticus. AJNR Am J Neuroradiol 40, 238–244.

Takeoka, M., Kim, F., Caviness Jr., V.S., Kennedy, D.N., Makris, N., Holmes, G.L., 2003. MRI volumetric analysis in rasmussen encephalitis: a longitudinal study. Epilepsia 44, 247–251.

C. Tang G. Luan T. Li Rasmussen's encephalitis: mechanisms update and potential therapy target Ther Adv Chronic Dis 11 2020 2040622320971413.

Tessonnier, L., Thomas, P., Benisvy, D., Chanalet, S., Chaborel, J.P., Bussiere, F., Darcourt, J., 2009. Perfusion SPECT findings in a suspected case of Rasmussen encephalitis. J Neuroimaging 19, 378–380.

Tripathi, P.P., Bozzi, Y., 2015. The role of dopaminergic and serotonergic systems in neurodevelopmental disorders: a focus on epilepsy and seizure susceptibility. Bioimpacts 5, 97–102.

Tzourio-Mazoyer, N., Landeau, B., Papathanassiou, D., Crivello, F., Etard, O., Delcroix, N., Mazoyer, B., Joliot, M., 2002. Automated anatomical labeling of activations in SPM using a macroscopic anatomical parcellation of the MNI MRI single-subject brain. NeuroImage 15, 273–289.

Varadkar, S., Bien, C.G., Kruse, C.A., Jensen, F.E., Bauer, J., Pardo, C.A., Vincent, A., Mathern, G.W., Cross, J.H., 2014. Rasmussen's encephalitis: clinical features, pathobiology, and treatment advances. Lancet Neurol 13, 195–205.

Wagner, J., Schoene-Bake, J.C., Bien, C.G., Urbach, H., Elger, C.E., Weber, B., 2012. Automated 3D MRI volumetry reveals regional atrophy differences in Rasmussen encephalitis. Epilepsia 53, 613–621.

Wang, D., Blumcke, I., Gui, Q., Zhou, W., Zuo, H., Lin, J., Luo, Y., 2013. Clinico-pathological investigations of Rasmussen encephalitis suggest multifocal disease progression and associated focal cortical dysplasia. Epileptic Disord 15, 32–43.

Wang, Z.I., Krishnan, B., Shattuck, D.W., Leahy, R.M., Moosa, A.N., Wyllie, E., Burgess, R.C., Al-Sharif, N.B., Joshi, A.A., Alexopoulos, A.V., Mosher, J.C., Udayasankar, U., Pediatric Imaging, N., Genetics, S., Jones, S.E., 2016. Automated MRI Volumetric Analysis in Patients with Rasmussen Syndrome. AJNR Am J Neuroradiol 37, 2348–2355.

Wilke, M., Altaye, M., Holland, S.K., Consortium, C.A., 2017. CerebroMatic: A Versatile Toolbox for Spline-Based MRI Template Creation. Front Comput Neurosci 11, 5.

Yamazaki, E., Takahashi, Y., Akasaka, N., Fujiwara, T., Inoue, Y., 2011. Temporal changes in brain MRI findings in Rasmussen syndrome. Epileptic Disord 13, 229–239.